

The residence time of focal adhesion kinase (FAK) and paxillin at focal adhesions in renal epithelial cells is determined by adhesion size, strength and life cycle status

Sylvia E. Le Dévédec¹, Bart Geverts², Hans de Bont¹, Kuan Yan³, Fons J. Verbeek³, Adriaan B. Houtsmuller^{2,*} and Bob van de Water^{1,*,‡}

¹Division of Toxicology, Leiden/Amsterdam Center for Drug Research, Leiden University, Leiden, Gorlaeus Laboratoria, PO Box 9502, 2300 RA Leiden, The Netherlands

²Department of Pathology, Josephine Nefkens Institute, Erasmus MC, University Medical Center, Rotterdam, PO Box 1738, 3000 DR Rotterdam, The Netherlands

³Imaging and Bioinformatics, Leiden Institute of Advanced Computer Science, Leiden University, Leiden, The Netherlands

*These authors contributed equally to this work

‡Author for correspondence (b.water@iacr.leidenuniv.nl)

Accepted 28 May 2012

Journal of Cell Science 125, 4498–4506

© 2012. Published by The Company of Biologists Ltd

doi: 10.1242/jcs.104273

Summary

Focal adhesions (FAs) are specialized membrane-associated multi-protein complexes that link the cell to the extracellular matrix and enable cell proliferation, survival and motility. Despite the extensive description of the molecular composition of FAs, the complex regulation of FA dynamics is unclear. We have used photobleaching assays of whole cells to determine the protein dynamics in every single focal adhesion. We identified that the focal adhesion proteins FAK and paxillin exist in two different states: a diffuse cytoplasmic pool and a transiently immobile FA-bound fraction with variable residence times. Interestingly, the average residence time of both proteins increased with focal adhesion size. Moreover, increasing integrin clustering by modulating surface collagen density increased residence time of FAK but not paxillin. Finally, this approach was applied to measure FAK and paxillin dynamics using nocodazole treatment followed by washout. This revealed an opposite residence time of FAK and paxillin in maturing and disassembling FAs, which depends on the ventral and peripheral cellular position of the FAs.

Key words: Focal adhesion, FRAP, FLIP

Introduction

Focal adhesions (FA) are transient structures essential in cell adhesion, spreading and migration as well as signaling for cell proliferation and survival (Berrier and Yamada, 2007; Webb et al., 2002; Webb et al., 2003; Zaidel-Bar et al., 2004; Zamir and Geiger, 2001). At FAs the extracellular matrix (ECM), including fibronectin and collagen, is linked to the actin cytoskeleton through clustered integrins and a complex network of cytoskeletal, adaptor, and signaling proteins, suggested to exist of at least 150 components, together referred to as the ‘integrin adhesome’ (Berrier and Yamada, 2007). Steady-state and motile cells can exhibit different types of adhesion such as focal adhesions, fibrillar adhesions or focal complexes (Zamir and Geiger, 2001b). Matrix adhesion sites are highly dynamic which is manifested by their assembly, disassembly and translocation (Webb et al., 2002; Webb et al., 2003). Since most components of FAs contain multiple binding sites for other components, the molecular complex may be assembled in numerous different ways giving rise to many different supramolecular structures but their function and kinetics are still unknown (Zaidel-Bar et al., 2004; Zamir and Geiger, 2001).

The non-receptor tyrosine kinase associated with FAs (focal adhesion kinase; FAK) and the adapter protein paxillin are two

well-known focal adhesion-associated proteins that are crucial in cell adhesion, migration and invasion (Webb et al., 2004). Both proteins are thought to have numerous interactions within the ‘integrin adhesome’ network (Zaidel-Bar et al., 2007a). Upon integrin binding to the ECM, FAK is recruited to FAs and autophosphorylated at tyrosine residue 397 and subsequently phosphorylated by Src at other tyrosine residue, thereby enabling dynamic restructuring of FAs (Schaller et al., 1994). Paxillin is a structural adaptor protein important in integrin signaling and interacts with FAK and, similar to FAK, with numerous other FA assembly proteins (Turner, 2000a; Turner, 2000b). It is phosphorylated on different Ser, Thr and Tyr residues, of which phosphorylation by the FAK/Src complex is essential in cell migration (for a review, see Deakin and Turner, 2008). Given the importance of both FAK and paxillin in FA organization and dynamics, further understanding of the molecular behavior of these proteins in individual focal adhesions and the physical-chemical factors that determine the dynamics is important.

Advances in fluorescent probes including genetically encoded fluorescent fusion proteins and imaging technologies have opened the door to studying dynamic cellular processes in living cells. Ideally, for each molecular entity in the cell, one

would like to know its concentration, aggregation state, interactions and dynamics in different locations within the cell at different times. Fluorescence recovery after photobleaching (FRAP) is an imaging technique that can be used to measure protein mobility in living cells, including binding and unbinding rate constants from immobile structures like, for example, focal adhesions or chromatin (Phair and Misteli, 2001; Houtsmuller and Vermeulen, 2001). FRAP is often used to measure protein exchange dynamics at cell-substrate adhesions but generally report only the half-time of fluorescence recovery ($t_{1/2}$). Here we applied a powerful and reliable photobleaching methodology that provides both spatial and temporal information on protein dynamics in FAs in a single cell. We employed simultaneous fluorescence loss in photobleaching (FLIP)-FRAP (Mattern et al., 2004), combined with Monte-Carlo simulation to fit the data and extract protein mobility parameters including diffusion rate and residence times at focal adhesions (Mattern et al., 2004). We applied the protocol to quantitatively assess FAK and paxillin protein mobility parameters in non-migrating renal proximal tubular epithelial cells. Although FAK and paxillin have an equal bound fraction at the focal adhesions, FAK resided for a shorter period (60 s) in focal adhesions than paxillin (100 s). Classification of FAs by size showed that residence time for both proteins increased in larger FAs. Furthermore, increasing integrin ligand interaction by modulating collagen density significantly prolonged the residence time of FAK while for paxillin the residence time decreased on high collagen concentration. Finally the use of nocodazole to initiate the assembly and maturation of focal adhesions and its removal to induce adhesion disassembly revealed the different behavior pattern of FAK and paxillin in ventral and peripheral located FAs, indicative for a complex regulation of protein dynamics.

Results

Mobility of GFP-FAK and GFP-paxillin in the cytosol and at focal adhesions of living cell

Focal adhesion dynamics is observed during acute renal ischemia/reperfusion injury in proximal tubular cells (Alderliesten et al., 2007). To further study the dynamics of the focal adhesion associated proteins FAK and paxillin, we used the renal epithelial cell line LLC-PK1, a well characterized cell line adherently growing on rigid planar substrate characterized by prominent matrix adhesions that are abundant and quite large in shape (van de Water et al., 2001). To study the behavior of FAK and paxillin in matrix adhesions, we generated LLC-PK1 cell lines ectopically expressing either GFP-FAK or GFP-paxillin, in which expression levels were similar to the endogenous counterparts and predominantly located at focal adhesions in living cells, showing their functionality in presence of the GFP tag (supplementary material Fig. S1A,B). LLC-PK1 cells expressing GFP or GFP-actin were used as controls. Importantly, live cell imaging demonstrated that GFP-FAK and GFP-paxillin containing FAs remain stable over a time period of 15 min (supplementary material Fig. S1C), allowing a reliable time scale of 5 min to study the kinetics of GFP-FAK and GFP-paxillin by FRAP.

First we investigated the cytoplasmic mobility of GFP-FAK and GFP-paxillin by photo-bleaching a thin strip spanning the width of the cytoplasm and recording the recovery of fluorescence in that strip (e.g. Houtsmuller, 2005). Analysis of the resulting recovery curves revealed that the majority of GFP-FAK and GFP-paxillin molecules were freely and equally mobile

in the cytoplasm, but slower than GFP only (supplementary material Fig. S2A). Next, association of GFP-FAK and GFP-paxillin with focal adhesions was assessed by bleaching a small region covering a single focal adhesion (supplementary material Fig. S2B,C). The recovery curves indicated fast but different exchange rates of FAK and paxillin with focal adhesions. This is in sharp contrast to the dynamics of GFP-actin, which showed hardly any recovery even after 1 min (supplementary material Fig. S2B).

Quantitative analysis of photobleaching experiments

Photobleaching experiments on single FAs are time consuming, and only a limited amount of FAs can be measured in one single cell. In order to obtain a sufficiently large data set to be able to quantitatively analyze FRAP experiments, we performed complementary simultaneous FLIP (fluorescence loss in photobleaching)-FRAP bleaching assays, (half-FRAP) which has been previously used to study protein exchange in small structures inside the cell nucleus in whole cells (Essers et al., 2002; Farla et al., 2004; Farla et al., 2005; Mattern et al., 2004). Note that in contrast to other FLIP applications, we apply a single bleach pulse to half of the cell and after that monitor both the fluorescence recovery rate in the bleached zone (FRAP) and the loss of fluorescence in the non-bleached half (FLIP). This technique is not the standard FLIP where a region is subjected to continuous bleaching while the fluorescence loss is monitored in a non-bleached region (Essers et al., 2002; Mattern et al., 2004) (for a review see van Royen et al., 2009). This adapted method has the advantage that all the structures of interest in a single cell can be analyzed. Moreover, combined analysis of FLIP and FRAP curves limits potential errors due to loss of fluorescence by the bleached pulse and by monitor bleaching. We first applied FLIP-FRAP to GFP-FAK cells. In less than 6 s half of the cell was bleached. Fluorescence recovery in the bleached half (FRAP) and loss of fluorescence in the unbleached half (FLIP) was monitored over a time period of 5 min with intervals of 6 s. Next, redistribution of fluorescence was analyzed at focal adhesions and in the cytoplasm of the GFP-FAK cells (Fig. 1A; supplementary material Movie 1). Focal adhesions localized at the cell periphery only (peripheral FAs) were all selected by image segmentation for further analysis (see supplementary material Fig. S3A,B for analysis example). Each bleached and unbleached half of the cytoplasm was divided in three regions of 50 pixels each (Fig. 1A; supplementary material Fig. S3A). FLIP and FRAP curves of individual focal adhesions located in each region were then averaged (Fig. 1B; supplementary material Fig. S3C) and the difference in relative fluorescence intensity between the averaged FLIP and the FRAP curves was then used for quantitative analysis (Fig. 1C). Typically, in one time-lapse series more than 50 focal adhesions in a single cell were analyzed in this way. The FLIP-FRAP curves decayed faster in the region close to the edge of the bleached region than in the distant regions, as expected (Fig. 1C).

FAK and paxillin diffuse similarly in the cytoplasm but associate with focal adhesion in two distinct kinetic pools

To further analyze and fit the experimental FLIP-FRAP data with a Monte-Carlo simulation, we obtained several z-scans of living LLC-PK1 expressing different GFP-tagged proteins cells (Fig. 2A) to generate a schematic cell model which had an average length of $\sim 60 \mu\text{m}$, width of $\sim 40 \mu\text{m}$ and height of $\sim 30 \mu\text{m}$ (Fig. 2B). A cell model was designed based on two

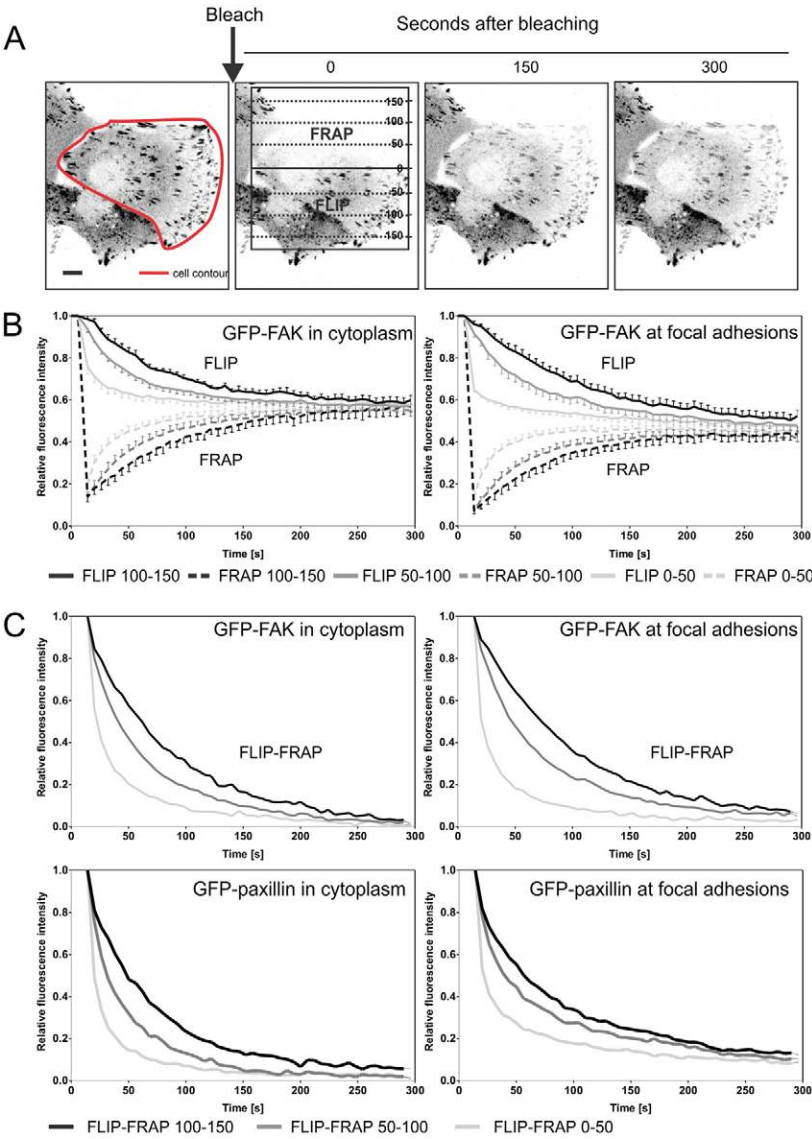


Fig. 1. Simultaneous FLIP-FRAP (=half-FRAP) of focal-adhesion-bound GFP-FAK and GFP-paxillin. (A) FLIP-FRAP on living LLC-PK1 cells expressing GFP-FAK. Cells are photobleached over a region covering about one half of the cell (indicated by black boxes). The images were acquired before bleaching and at 6-s intervals after bleaching, starting at 0 s. Scale bar: 10 μ m. Images were inverted for easy visualization. (B) Quantitative analysis of redistribution of GFP-FAK in the cytoplasm and at focal adhesions separately in the bleached and unbleached half of the cell (and in the three different regions 0–50, 50–100 and 100–150 pixels). Values are means \pm s.e.m. from at least 300 adhesions per curve measured in about 25 cells on five different days. (C) Differences in GFP intensity in bleached and unbleached parts of the cell (=FLIP-FRAP) calculated from the data shown in B for GFP-FAK and also for GFP-paxillin.

ellipsoids to represent cytoplasm and nucleus (where GFP-paxillin and GFP-FAK are considered not present; Fig. 2C). We also assigned a number of objects located in the six different regions (FRAP and FLIP at 0–50, 50–100, 100–150 pixels) that represent the focal adhesions at the bottom of the cell (Fig. 2C). This LLC-PK1 cell model was used in a Monte-Carlo computer simulation to generate curves in which diffusion as well as association and dissociation rates to and from focal adhesions were systematically varied. Recovery curves of the cytoplasmic fluorescence of both GFP-paxillin and -FAK indicate equal diffusion of both proteins (Fig. 1C). Indeed, the GFP-FAK and GFP-paxillin data fitted best to simulated curves with a diffusion coefficient of 4 μ m²/s. Free cytoplasmic GFP showed a faster recovery with diffusion coefficient of 15 μ m²/s, clearly higher than that of GFP-FAK and GFP-paxillin (data not shown). We then calculated the ratio between total focal adhesion and total cytoplasmic fluorescence. Indeed, our automated analysis of the movies provides us with the average pixel intensity for each segmented object (either FA or cytoplasmic regions manually drawn). Because GFP fluorescence intensity is

proportional to GFP-FAK or GFP-paxillin concentration, this ratio should give a good estimate of the fraction of GFP-FAK and GFP-paxillin bound to the focal adhesions. The average intensity for GFP-FAK and GFP-paxillin at the focal adhesions although different from each other was both \sim 2.7 times higher than in the cytoplasm indicating that FAK and paxillin are present in similar quantities in focal adhesions. Simultaneous FLIP-FRAP analysis indicated that GFP-FAK is almost completely redistributed over bleached and unbleached focal adhesions within 5 min after bleaching (Fig. 1B,C). In contrast, GFP-paxillin redistribution is not complete within this time interval (Fig. 1C; supplementary material Fig. S3C). Fitting of the experimental GFP-FAK data to curves generated by computer simulation assuming simple binding kinetics, indicated a characteristic residence time of \sim 60 s at the focal adhesions whereas GFP-paxillin had a characteristic residence time of \sim 120 s. These data show that although present in similar amounts, the dynamics of the partners FAK and paxillin are different from each other and that FAK has a faster turnover at FA sites than paxillin.

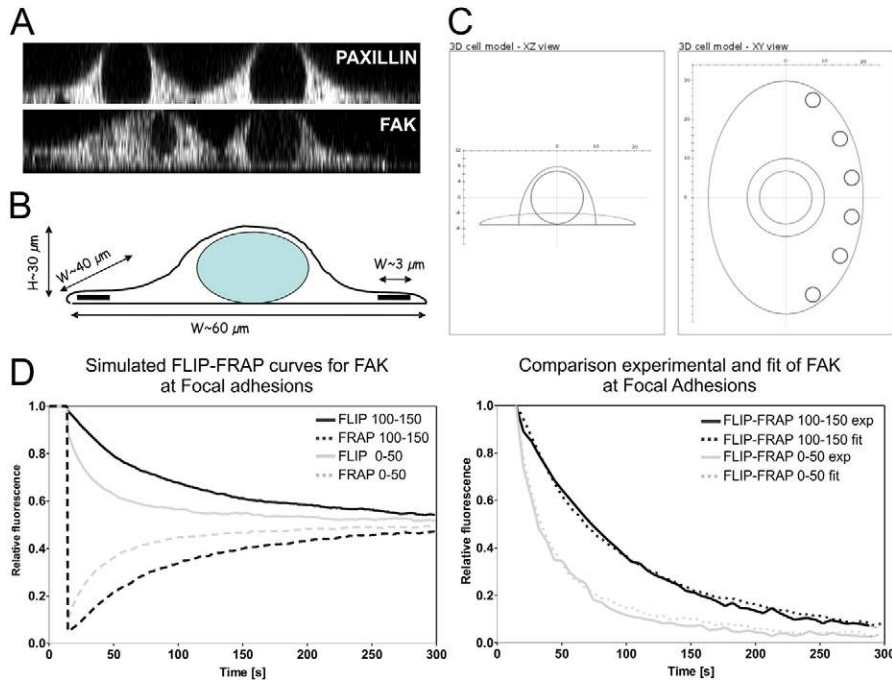


Fig. 2. The 3D cell model used for the Monte-Carlo simulation. (A) Z-scan projection of LLC-PK1 cells expressing GFP-paxillin and GFP-FAK. (B) Schematic view of a LLC-PK1 cell in a steady state. (C) 3D cell model used for Monte-Carlo simulation. Two ellipsoids represent the cytoplasm and an empty ball represents the nucleus. The circular structures represent focal adhesions located in the different FLIP-FRAP regions. (D) Fitting analysis of experimental data from FLIP-FRAP curves representing the regions of 0–50 and 100–150 pixels for FA-associated paxillin and FAK.

Increased residence time of FAK and paxillin is correlated with focal adhesion size

We then analyzed whether the mobility of FAK and paxillin is related to FA size (Fig. 3A). We categorized the focal adhesions in three sizes based on surface areas: $0\text{--}1 \mu\text{m}^2$, $1\text{--}3 \mu\text{m}^2$, $3\text{--}15 \mu\text{m}^2$. GFP-FAK and GFP-paxillin cells showed comparable FA size distributions (Fig. 3B). Analysis of the FLIP-FRAP curves (Fig. 3C,D) of FAK and paxillin in FAs of different sizes showed a clear correlation between residence times and focal adhesion size. Interestingly, the residence time of FAK as well as paxillin in large focal adhesions was twofold higher compared to the smaller adhesions (Fig. 3E). The residence time of paxillin was consistently higher than FAK at all adhesion areas (Fig. 3E). These data show that in the periphery of the cell FAK and paxillin protein dynamics was much slower in large focal adhesions than in small ones.

Paxillin and FAK dissociation from focal adhesions correlates with adhesion strength

The number of focal adhesions, their size, distribution and dynamics is dependent on ECM composition and density (Katz et al., 2000). Here we determined whether ECM density affects the residence time of FAK and paxillin at focal adhesions (Katz et al., 2000; Li et al., 2005). LLC-PK1 cells expressing GFP-FAK or GFP-paxillin were plated on different collagen densities (1, 10, 100 μg collagen/ml, abbreviated C1, C10 and C100). At 100 μg collagen/ml, LLC-PK1 cells did not fully spread compared to the lowest 1 and 10 μg collagen/ml (Fig. 4A). Moreover, under these conditions, cells had only peripheral FAs that were large in size and always associated with thick peripheral F-actin bundles (Fig. 4A). There was no difference in number of adhesions from low to high collagen concentration except for GFP-FAK cells where the number of small adhesions was smaller on C1 than C10 (Fig. 4Ba,b). FLIP-FRAP experiments on both GFP-FAK and GFP-paxillin cells at 1, 10 and 100 μg collagen/ml concentrations showed that the residence time of paxillin was significantly affected by ECM substrate density especially on the

high density where the paxillin dynamics was faster than on the low collagen concentration (Fig. 4Ca; supplementary material Fig. S4A,B). On the contrary, the residence time of FAK at focal adhesions increased with higher collagen density by twofold (Fig. 4Cb), indicating that increasing adhesion strength correlates with a longer residence time of FAK. The localization of P-Tyr397-FAK at focal adhesions was similar on the three collagen concentration (supplementary material Fig. S5A). Yet the focal adhesion associated P-Tyr31/118-paxillin was not present on all focal adhesions (supplementary material Fig. S5C). These data indicate that adhesion strength regulates focal adhesion proteins turnover with different regulatory components for FAK and paxillin.

Adhesion protein turnover depends on the cellular location and the phase of the adhesion life cycle

To determine how the kinetics of FAK and paxillin are affected during adhesion assembly and disassembly, we performed the so-called nocodazole assay that disrupts the microtubules thereby allowing local focal adhesion maturation, while upon nocodazole washout and microtubule built up, focal adhesions are disassembled (Ezratty et al., 2005) (supplementary material Fig. S6A). This assay was combined with our FRAP-FLIP approach. Cells exposed to 10 μM of nocodazole (NOCO) showed increased contractility while removal of nocodazole (washout, WO) resulted in decreased contractility of the actin cytoskeleton. Indeed, phalloidin staining in control (DMSO), NOCO and WO cells showed increase in F-actin stress fibers (thicker and shorter) than span over the ventral face of the cell and that will again disappear upon washout (=regrowth of the microtubules) of the nocodazole (Fig. 5A). Therefore, we added another category of adhesions: either localized at the cell periphery (peripheral) or on the ventral face of cells around the nucleus (ventral; Fig. 5B). We sorted again the different FA structures based on their area ($0\text{--}1 \mu\text{m}^2$, $1\text{--}3 \mu\text{m}^2$ and $3\text{--}15 \mu\text{m}^2$). Immunolocalization of PY epitopes revealed the increased number and enlargement of the FA after microtubule

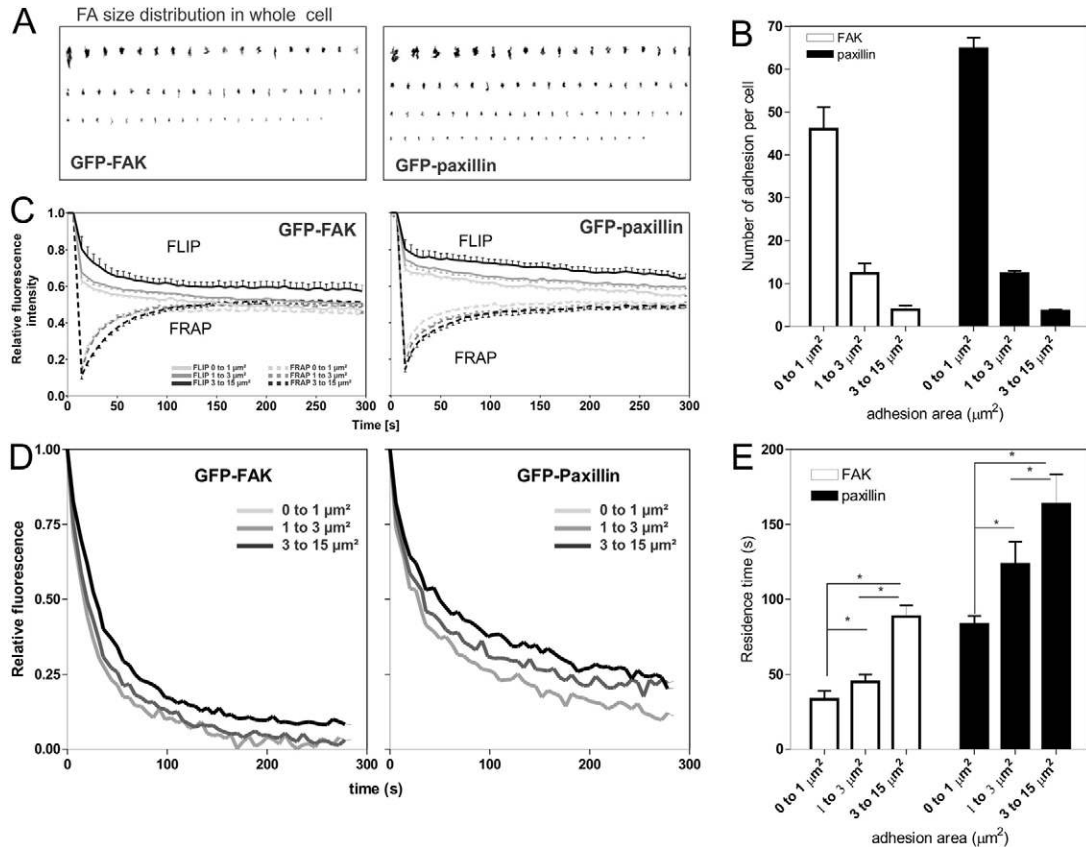


Fig. 3. Focal adhesion size is a function of FAK and paxillin residence time. (A) Examples of the variety of matrix adhesions in cells expressing GFP-FAK and GFP-paxillin. After image segmentation based on intensity threshold over the whole cell, focal adhesions can be displayed according to their size using Image-Pro-Plus software; individual focal adhesion images were inverted for easy visualization. (B) Plot showing the number of adhesions per cell versus adhesion size (μm^2). Measurements were done on five sets of data collected on different days with five to six cells per cell line. Values are means \pm s.e.m. (C) Quantitative analysis of redistribution of GFP-FAK (left) and GFP-paxillin (right) at focal adhesions separately in the bleached and unbleached halves of the cell after sorting according to focal adhesion size (small: 0–1 μm^2 ; medium: 1–3 μm^2 ; large: 3–15 μm^2). Values are means \pm s.e.m. FRAP experiments were performed on ~25 cells on five different days. For GFP-FAK 343 small (0–1 μm^2), 114 medium (1–3 μm^2) and 33 large (3–15 μm^2) adhesions were analyzed, in the region 0–50 pixels. (D) FLIP-FRAP curves of GFP-FAK and GFP-paxillin sorted according to the adhesion area. For GFP-FAK, 343 small (0–1 μm^2), 114 medium (1–3 μm^2) and 33 large (3–15 μm^2) adhesions were analyzed and for GFP-paxillin, 409 small (0–1 μm^2), 95 medium (1–3 μm^2) and 33 large (3–15 μm^2) adhesions were analyzed, in the region 0–50 pixels. (E) Plot showing residence time of both FAK and paxillin versus adhesion area (μm^2). Values are means \pm s.e.m. * $P < 0.05$ based on the bootstrap hypothesis test.

disruption (Fig. 5A; supplementary material Fig. S6C,D). The presumed NOCO-induced contractile switching of the cells was supported by western blot analysis of p-Ser190MLC: NOCO exposure caused an increase of pSer190-MLC, and NOCO/WO caused a dephosphorylation of pSer190-MLC (supplementary material Fig. S6B). The localization of P-Tyr397-FAK at focal adhesions was similar during the assay while P-Tyr31/118-paxillin was absent at focal adhesions during WO (supplementary material Fig. S7). We performed our half-FRAP experiment on control cells exposed to DMSO, cells exposed to NOCO for 120 min and cells that received 30 min NOCO and washout. This resulted in a complex map of kinetics for both FAK and paxillin proteins at focal adhesion depending their size, location and treatment condition. Thus, on the ventral side of the cell FAK and paxillin showed in most cases a similar behavior: faster turnover during NOCO and WO (Fig. 5Da,b). Of notice, FAK disassociation was as fast as diffusion when the medium adhesions disappeared during WO (Fig. 5Db). Large ventral focal adhesion were only observed during NOCO treatment, and most likely rapidly disassembled

during WO. On the periphery of the cells, the 2-fold difference in residence time between FAK and paxillin was present under DMSO control conditions (Fig. 5Ca,b). Interestingly, NOCO treatment caused an increase in the residence time of FAK in peripheral small focal adhesions, while the paxillin residence time decreased to almost equal the residence time of FAK (Fig. 5Ca,b). Also in small peripheral focal adhesions, these opposite directional changes in the residence times of FAK and paxillin were still observed during the WO phase. Yet for medium-sized focal adhesions, the residence time of FAK was again drastically reduced (Fig. 5Cb). These data underscore the complexity of the regulation of proteins within focal adhesions, and highlight the importance to perform half-FRAP when unraveling mechanisms of protein dynamics at focal adhesions.

Discussion

Understanding the molecular mechanisms that orchestrate the dynamics of focal adhesions is necessary to improve our insight in fundamental processes such as cell survival, proliferation and

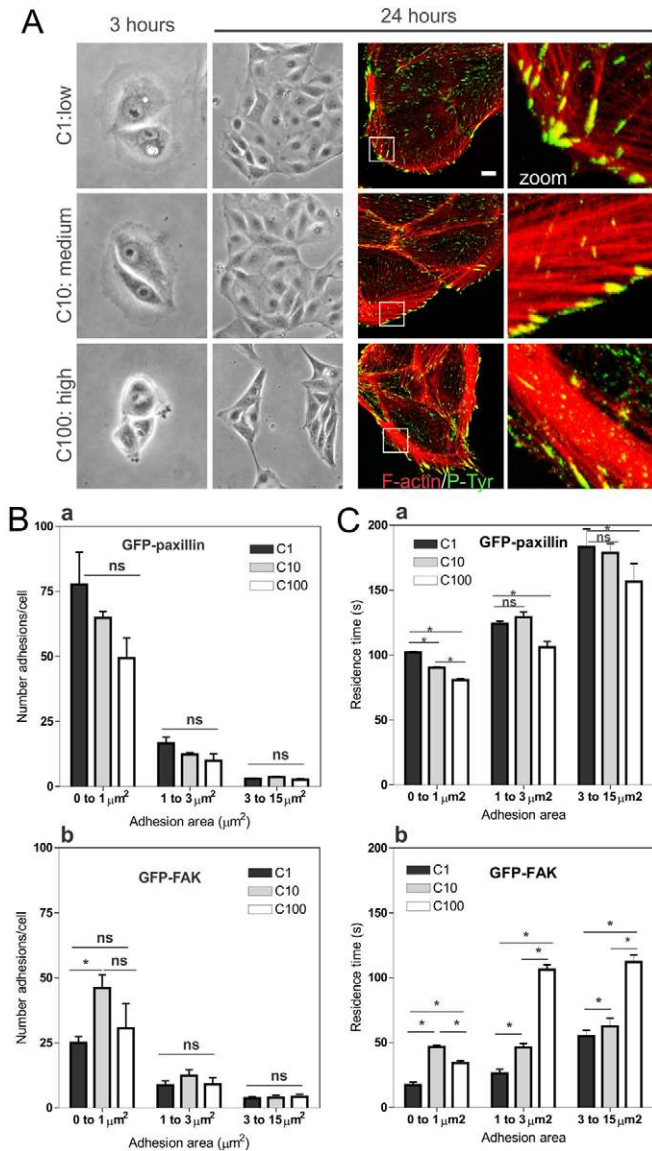


Fig. 4. FAK and paxillin residence times are regulated by ligand density. (A) LLC-PK1 cells 3 h and 24 h after plating on coverslips coated with the indicated concentrations of collagen (C1: 1 $\mu\text{g}/\text{ml}$, C10: 10 $\mu\text{g}/\text{ml}$ and C100: 100 $\mu\text{g}/\text{ml}$) with F-actin-phalloidin (red) and phosphotyrosine (green) shown in the merged images. Scale bar: 10 μm . The right column shows enlarged images of the boxed regions. (B) Plot showing the number of adhesions per cell [GFP-paxillin (a) and GFP-FAK (b)] plated on low, medium and high collagen versus adhesion size (μm^2). Measurements were performed on four sets of data collected at different days with five to six cells per cell line. Values are means \pm s.e.m. * $P < 0.05$ based on the Student's *t*-test. (C) Plot showing residence time of GFP-paxillin (a) and GFP-FAK (b) versus collagen concentration and adhesion area. For GFP-FAK and GFP-paxillin, the experiment was performed on three different days. GFP-FAK (C1, 16 cells, $n_{\text{small}}=107$, $n_{\text{medium}}=44$, $n_{\text{large}}=18$; C10, 15 cells, $n_{\text{small}}=238$, $n_{\text{medium}}=67$, $n_{\text{large}}=20$; C100, 18 cells, $n_{\text{small}}=157$, $n_{\text{medium}}=46$, $n_{\text{large}}=20$). GFP-paxillin (C1, 17 cells, $n_{\text{small}}=466$, $n_{\text{medium}}=107$, $n_{\text{large}}=10$; C10, 15 cells, $n_{\text{small}}=232$, $n_{\text{medium}}=41$, $n_{\text{large}}=2$; C100, 17 cells, $n_{\text{small}}=133$, $n_{\text{medium}}=36$, $n_{\text{large}}=19$). * $P < 0.05$ based on the bootstrap hypothesis test.

migration. In the present study, we have developed and used a fast and reliable adapted photobleaching methodology (FLIP-FRAP) combined with Monte-Carlo simulation to determine the behavior of individual focal adhesion components at cell matrix

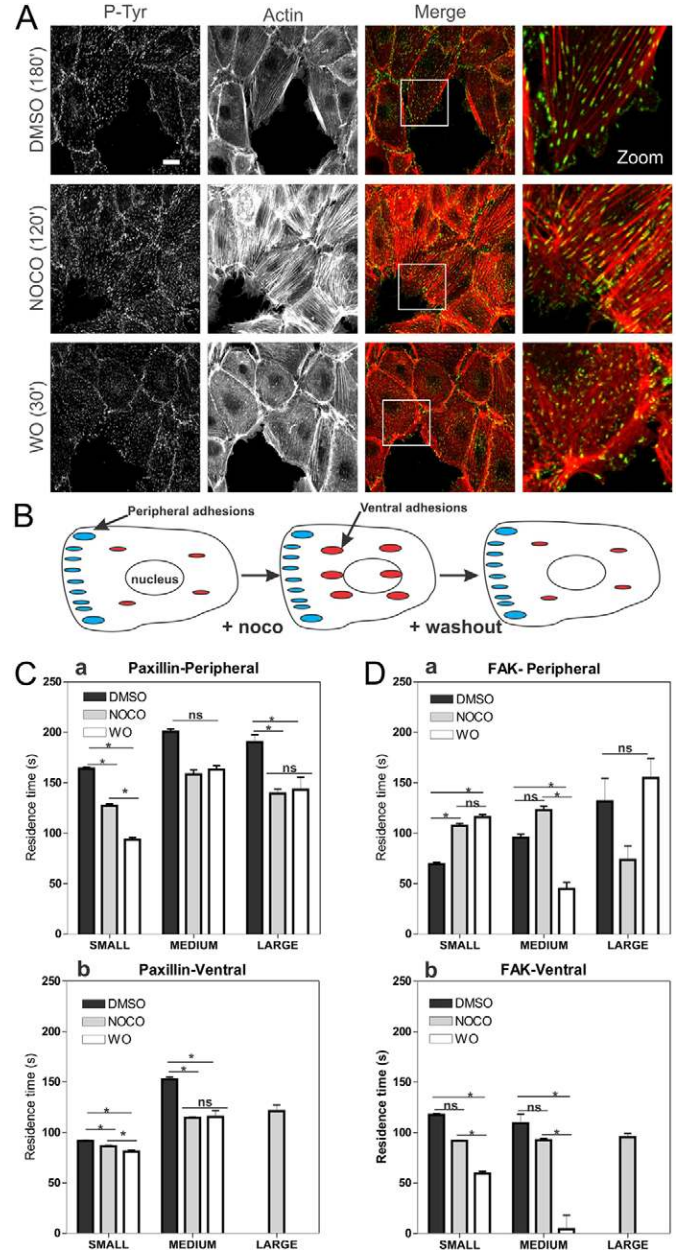


Fig. 5. Dynamics of FAK and paxillin during adhesion assembly and disassembly in the nocodazole assay. (A) F-actin-phalloidin and phosphotyrosine immunostaining of LLC-PK1 cells exposed to DMSO for 180 min, nocodazole (10 μM) for 120 min and washout for 30 min (after nocodazole exposure). (B) Schematic view of the peripheral and ventral adhesions as they were segmented in the FRAP experiments. (C) Plot showing residence time of GFP-paxillin when localized in either peripheral (a) or ventral (b) adhesions during the nocodazole assay (sorted on size). 30 cells were analyzed over six different days for the DMSO condition ($n_{\text{periph}}=639$; $n_{\text{ventral}}=1017$). 31 cells were analyzed for the NOCO condition ($n_{\text{periph}}=622$; $n_{\text{ventral}}=1487$). 24 cells were analyzed for the WO condition ($n_{\text{periph}}=748$; $n_{\text{ventral}}=789$). (D) Plot showing residence times of GFP-FAK when localized in either peripheral (a) or ventral (b) adhesions during the nocodazole assay (sorted on size). 27 cells were analyzed over six different days for the DMSO condition ($n_{\text{periph}}=612$; $n_{\text{ventral}}=617$). 26 cells were analyzed for the NOCO condition ($n_{\text{periph}}=527$; $n_{\text{ventral}}=1256$). 20 cells were analyzed for the WO condition ($n_{\text{periph}}=490$; $n_{\text{ventral}}=483$). * $P < 0.05$ based on the bootstrap hypothesis test.

adhesion complexes within living cells. We applied this technique to determine the dynamic behavior of FAK and paxillin, two important focal adhesion proteins, in the cytoplasm and within focal adhesions in stationary epithelial cells plated on collagen, on increasing adhesion strength and in dynamic focal adhesions after microtubule depolymerization (Ezratty et al., 2005). Our data indicate that: (1) FAK and paxillin exist in two different states: a fast diffusing cytoplasmic pool in concordance with previous measurements (Digman et al., 2005; Wolfenson et al., 2009), and a transiently immobile FA-bound fraction with variable residence times; (2) residence time of both FA proteins increases with increasing FA size; (3) adhesion strength modified by modulating ECM ligand density increases the time of residence at FAs of FAK but not paxillin; and (4) the dynamics of FAK and paxillin can be modulated in different directions depending on the phase of the life cycle of focal adhesions.

So far FRAP has been used to study adhesion protein kinetics to determine the $t_{1/2}$ value at individual FA without integrating any spatial resolution (Cluzel et al., 2005; Edlund et al., 2001; Geuijen and Sonnenberg, 2002; Giannone et al., 2004; Hamadi et al., 2005; Lele et al., 2006; Pasapera et al., 2010). Our half-FRAP/Monte-Carlo simulation approach uses a three-dimensional cell model derived from experimental data, and can be used to determine protein mobility parameters based on the majority of the focal adhesions in a single cell. This provides the possibility to map protein parameters according to the focal adhesion size and distribution over the cell body.

We showed that GFP-FAK and GFP-paxillin diffuses through the cytoplasm and did not detect any directed movement towards FAs. GFP-FAK and GFP-paxillin show the same diffusion coefficient suggesting that FAK and paxillin may move together in the cytoplasm in larger complexes but FRAP experiment cannot reveal direct binding. However, very recent ccRICS data obtained by Choi and colleagues demonstrated that in fact, fluorescently tagged paxillin and FAK molecules diffuse independently in the cytosol and do not form complexes before entering adhesions. Wild-type paxillin and FAK reside in complexes only within nascent adhesions and this association can be enhanced by phosphorylation of paxillin on residues Y31 and Y118 (Choi et al., 2011).

Our FRAP-data show that in resting renal cells FAK and paxillin are transiently immobilized to focal adhesions with residence time of ~60 s and 120 s, respectively. This fold difference in behavior between FAK and paxillin is in the same order of magnitude as observed in capillary endothelial cells or in mouse embryonic fibroblasts using only FRAP and mathematical modeling [~10 s for FAK and ~25 s for paxillin (Lele et al., 2008; Pasapera et al., 2010)]. Interestingly, we observed that FAK and paxillin have longer residence times in larger focal adhesions than in smaller focal adhesion. Despite the fact that FAK and paxillin both localize at focal adhesions, they clearly differ in their behavior. This can be explained by the differences in the set of focal adhesion binding partners of both proteins (Zaidel-Bar et al., 2007a). Thus, while paxillin has strong interaction with various structural components in focal adhesions (more than 30), including talin, ILK, Crk, PAK, tubulin and actin, FAK rather associates with signaling intermediates as well as some adapter proteins such as FAK itself, Src, p190Gap, calpain and others. Also, the binding property and kinase activity of FAK control its dynamics since FAK lacking its kinase domain shows increased exchange between FAs and cytosol (data not shown,

Giannone et al., 2004; Hamadi et al., 2005). Interestingly, during NOCO and WO treatment these dynamic behaviors of FAK and paxillin drastically change (see Fig. 5) which is indicative for modified local interactions with other proteins, most likely controlled by phosphorylation as shown earlier for vinculin (Möhl et al., 2009).

Our data indicate that adhesion strength is directly associated with FAK and paxillin transient immobilization in focal adhesions which was also demonstrated for vinculin in migrating cells (Möhl et al., 2009). In our model system the degree of ECM ligand density seems to determine intracellular tension (Fig. 4B). Several studies demonstrate that tension is an important determinant for adhesion size and molecular (phospho-) protein composition of FAs. In human foreskin fibroblasts, the tension generated by a focal adhesion correlates with focal adhesion size and with the local accumulation of the focal adhesion adaptor protein vinculin (Balaban et al., 2001). Moreover, cytoskeletal stiffness mediates increase in focal adhesion size and density along with changes in their molecular composition (Goffin et al., 2006), while localization and turnover of zyxin was tension dependent (Yoshigi et al., 2005; Zaidel-Bar et al., 2007b). In our nocodazole assay we also observed enhanced actin cytoskeletal built up associated with increased phosphorylation of myosin light chain, indicative for tension formation. This was associated with changes in the dynamics of FAK (slower) and paxillin (faster) in small focal adhesions in the periphery. Yet, in maturing ventral focal adhesions that are associated with the actin cytoskeleton, FAK dynamics became faster. We propose that the actin cytoskeletal organization and tension is an important determinant for local signaling events that thereby drive the dynamics of the focal adhesion-associated proteins.

In conclusion, our combined FLIP-FRAP approach allowed us to analyze the majority of focal adhesions in an individual cell with respect to type, size and distribution which can be correlated to the protein dynamics. The practicality and general applicability of this technique in a wide variety of settings should prove useful in further characterizing the regulation of matrix adhesions under different biological settings. A quantitative mapping of the residence times of all major FA-associated proteins in the entire cell according to its localization, size and type and in direct relation to the migratory behavior as well as their regulation by external signaling curves remains an important next challenge.

Materials and Methods

Cell lines

Here we used the porcine renal epithelial cell line LLC-PK1. Cells were maintained in DMEM supplemented with 10% (v/v) FCS and penicillin/streptomycin at 37°C in a humidified atmosphere of 95% air and 5% CO₂. Stable eGFP and eGFP-FAK have been described previously (van de Water et al., 2001). For preparation of stable GFP-expressing cell lines, LLC-PK1 cells were transfected with 0.8 µg DNA of pGZ21-paxillin and GFP-actin using Lipofectamine 2000 reagent according to the manufacturer's procedures (Life Technologies, Inc.). Stable transfectants were selected using 800 µg/ml G418. Individual clones were picked and maintained in complete medium containing 100 µg/ml G418. Clones were analyzed for paxillin expression using western blotting and immunofluorescence. For further experiments one representative stable cell lines was used per construct. For immunofluorescence studies, cells were cultured on collagen-coated glass coverslips in 24-well dishes and allowed to adhere overnight in complete culture medium. For live-cell microscopy, cells were plated on 35-mm glass coated with either 10 µg/ml collagen (control situation) or 1, 10 or 100 µg/ml collagen (for extracellular matrix density experiment) and let stretched in complete medium for overnight. Collagen type 1 from rat tail (Sigma-Aldrich) was stored at 3 mg/ml and diluted to the appropriate concentration for coating in PBS. In all cases, coating was done by incubation for 2 h at 37°C. Coated surfaces were washed three times with PBS and blocked with 1% heat denatured BSA in PBS for 1 h at 37°C.

Western blot analysis

For western blot analysis cells were washed twice with PBS and lysed in ice-cold lysis buffer [50 mM HEPES, 150 mM NaCl, 1% (w/v) NP40, 1 mM EDTA pH 7.4] plus inhibitors (2 mM AEBSF, 100 µg/ml aprotinin, 17 µg/ml leupeptin, 1 µg/ml pepstatin, 5 µM farnesylate, 5 µM BpVphen and 1 µM okadaic acid) for 5 min. After lysis, cells were scraped and centrifuged for 5 min at 4°C, 14,000 rpm. Protein concentrations were determined using Coomassie Protein Assay Reagent using IgG as a standard (Pierce). Equal amounts of protein were separated by SDS-PAGE and transferred to PVDF membrane (Millipore). Blots were blocked with 5% (w/v) BSA in TBS-T [0.15 M NaCl, 50 mM Tris-HCl and 0.05% (v/v) Tween-20] overnight at 4°C and probed with appropriate primary antibodies for 3 h at room temperature as follows: anti-FAK (monoclonal, 1 µg/ml, BD Transduction Labs), anti-paxillin (monoclonal, 0.5 µg/ml, BD Transduction Labs), anti-GFP (polyclonal, 1 µg/ml, Roche), and anti P-Ser190MLC (Santa Cruz).

Immunofluorescence

Cells were fixed with 3.7% formaldehyde for 10 min followed by three washes with PBS. After cell permeabilization and blocking with PBS/0.2% (w/v) Triton X-100/0.5% (w/v) BSA, pH 7.4 (PTB) cells were stained for P-Tyr397-FAK (BioSource), P-Tyr118-paxillin (BioSource), paxillin (BD Transduction Labs) diluted in TBP [0.1% (w/v) Triton X-100 and 0.5% (w/v) BSA in PBS, pH 7.4]. For secondary staining Cy3-labeled goat anti-mouse or anti-rabbit antibodies (Jackson Laboratories) were used. Cells were mounted on glass slides using Aquapoly-Mount (Polysciences Inc., Warrington, PA). Cells were viewed using a BioRad 2-photon confocal laser scanning microscope and images were processed with Image-Pro® Plus (Version 5.1; Media Cybernetics).

Image processing

For readers clarification, sometimes images are inverted so that for a 8 bit image, an intensity of 0 became 256 and an intensity of 256 become 0.

Live-cell microscopy, fluorescence recovery after photobleaching and fluorescence loss in photobleaching

Live-cell microscopy was performed with a Zeiss LSM 510 META confocal laser scanning microscope equipped with a heated (37°C) scan stage and a Plan-Apochromat oil immersion objective [40×, numerical aperture (NA) 1.3, for all FRAP procedures]. GFP fluorescence was detected by using the 488-nm line of a fiber-coupled 60-mW argon laser, a dichroic beamsplitter (488/543) and a 510- to 545-bandpass emission filter.

All FRAP procedures were performed with the same experimental set-up as for live-cell microscopy.

Strip-FRAP in cytoplasm

To determine cytoplasmic mobility of GFP, GFP-FAK and GFP-paxillin, a strip 1 µm wide spanning approximately the width of the cytoplasm (without any visible focal adhesion) was photobleached by a short bleach pulse (100 ms) at 100% laser intensity of a 60-mW argon laser at 488 nm. Recovery of fluorescence within the strip was monitored using 100-ms intervals and low laser intensity to avoid photobleaching by monitoring. Approximately 10 cells were averaged to generate one FRAP curve for a single experiment.

FRAP on individual focal adhesions

Spot bleaching was applied to a small area of 0.80 µm² covering a single focal adhesion for 1 s at a 50-µW laser intensity. Redistribution of fluorescence was monitored with 100 ms time intervals at low laser intensity starting directly after the bleach pulse. Images were analyzed by using LSM Image software (Zeiss). The relative fluorescence intensity of individual focal adhesion, was calculated at each time interval as follows: $I_{rel}(t) = (F_A(t) / F_{A0})$, where $F_A(t)$ is the intensity of the focal adhesion at time point t after bleaching, F_{A0} is the average intensity of the focal adhesion before bleaching. Approximately 15 focal adhesions (each in a distinct cell) were averaged to generate one FRAP curve for a single experiment, and the experiment was performed on at least three different days. The experimental data were fitted (least-squares best fit) to the following equation: $I_{rel}(t) = f_1(1 - e^{-k_1 t}) + f_2(1 - e^{-k_2 t})$, where f_1 and f_2 are the fractions and k_1 and k_2 are the corresponding rate constants of those fractions. Half lives were calculated as $t_{1/2} = \ln 2 / k$.

Combined FLIP-FRAP analysis in a single cell

For simultaneous FRAP and FLIP in a single cell, photobleaching was applied to about half the cell for less than 6 s at high laser intensity. Redistribution of fluorescence was monitored with 6 s time intervals. We processed the different time lapse movies using Image Pro software using in house written macro where focal adhesions were segmented based on intensity. Fluorescence intensity values over the time for each focal adhesion were exported into Excel together with FA morphologic parameters (size, elongation, area, localization). The difference between relative fluorescence intensities of bleached (FRAP) and unbleached (FLIP) focal adhesion was calculated as $I_{rel}(t) = [(F_A(t) - background) / (F_{A0} - background)]_{unbleached} - [(F_A(t) - background) / (F_{A0} - background)]_{bleached}$ and normalized to the first data point after bleaching. Approximately five cells with more than 50 focal adhesions per cell were averaged to

generate FRAP and FLIP curves for a single experiment, and the data shown were performed on at least three different days.

FRAP analysis

For analysis of FRAP data, FRAP curves were normalized to prebleach values and the best fitting curve (least squares) was picked from a large set of computer simulated FRAP curves in which three parameters representing mobility properties were varied: diffusion rate (ranging from 1 to 25 µm²/s), immobile fraction (0, 10, 20, 30, 40, 50%) and time spent in immobile state, ranging from 10, 20, 30, 40 s to ∞ s. Monte Carlo computer simulations used to generate FLIP and FRAP curves were based on a cell model of diffusion (ellipsoid volume representing the cytoplasm of the cell which includes another smaller ellipsoid volume representing the nucleus), and simple binding kinetics representing binding to immobile elements in the cell, representing focal adhesions (Fig. 3). Simulations were performed at unit time steps corresponding to the experimental sample rate of 5 s. Diffusion was simulated by each step deriving novel positions $M(x+dx, y+dy, z+dz)$ for all mobile molecules $[M(x, y, z)]$, where $dx = G(r_1)$, $dy = G(r_2)$ and $dz = G(r_3)$, r_i is a random number ($0 \leq r_i \leq 1$) chosen from a uniform distribution, and $G(r_i)$ is an inverse cumulative Gaussian distribution with $\mu = 0$ and $\sigma^2 = 2Dt$, where D is the diffusion coefficient and t is time measured in unit time steps. Immobilization was based on simple binding kinetics described by: $k_{on}/k_{off} = F_{imm}/(1 - F_{imm})$, where F_{imm} is the relative number of immobile molecules. The chance of each particle becoming immobilized per unit time (representing focal-adhesion-binding) was defined as $P_{immobilise} = k_{on} \times F_{imm}/(1 - F_{imm})$, where $k_{on} = 1/t_{imm}$, and t_{imm} is the average time spent in immobile complexes measured in unit time steps; the chance to release was $P_{mobilise} = k_{off} = 1/t_{imm}$. The FRAP procedure was simulated on the basis of an experimentally derived three-dimensional laser intensity profile providing a chance based on three-dimensional position for each molecule to be bleached during simulation of the bleach pulse.

Statistical analysis

Student's t -test was used to determine significant differences between two means ($P < 0.05$). For time-series data, the bootstrap hypothesis test (BHT), also known as a subcategory of permutation test, was used (Edgington, 1995; Good, 2005; Härdle et al., 2003). Bootstrap sampling is a data sampling technique for approximating empirical distribution in observed data (Efron and Tibshirani, 1993). Each experimental FLIP and FRAP curves data are used to calculate a standard FLIP-FRAP curve. By repeatedly applying the procedure, we obtain a set of FLIP-FRAP curves and the cumulative density of such set approximates the empirical distribution of FLIP-FRAP data at each time point. The required number of iterations is defined by the maximum size of either raw FLIP or FRAP data. The modified test statistic of BHT is implemented using Eqn 1, in which the \bar{x}^* is the mean vector of the first n observed vectors from sample population x , \bar{y}^* is the mean vector of the first m vectors from sample population y . The $\bar{\sigma}_x$ and $\bar{\sigma}_y$ are the standard deviation vectors from sample population x and y .

$$t = \frac{\sum_{j=1}^T (\bar{x}_j^* - \bar{y}_j^*)}{\sum_{j=1}^T \left(\sqrt{\frac{\bar{\sigma}_{xj}^2}{n} + \frac{\bar{\sigma}_{yj}^2}{m}} \right)} \quad (1)$$

Acknowledgements

We thank the imaging members of the Division of Toxicology for helpful suggestions and the IOC imaging center at Erasmus Rotterdam for technical support.

Funding

This work was supported by the Dutch Cancer Society [grant numbers UL 2006-3538, UL 2007-3860 both to B. v.d.W.]; and the European Union FP7 Metafight project [grant agreement number 201862 to B. v.d.W.].

Supplementary material available online at

<http://jcs.biologists.org/lookup/suppl/doi:10.1242/jcs.104273/-/DC1>

References

- Alderliesten, M., de Graauw, M., Oldenampsen, J., Qin, Y., Pont, C., van Buren, L. and van de Water, B. (2007). Extracellular signal-regulated kinase activation during renal ischemia/reperfusion mediates focal adhesion dissolution and renal injury. *Am. J. Pathol.* **171**, 452-462.
- Balaban, N. Q., Schwalz, U. S., Riveline, D., Goichberg, P., Tzur, G., Sabanay, I., Mahalu, D., Safran, S., Bershadsky, A., Addadi, L. et al. (2001). Force and focal

- adhesion assembly: a close relationship studied using elastic micropatterned substrates. *Nat. Cell Biol.* **3**, 466-472.
- Berrier, A. L. and Yamada, K. M. (2007). Cell-matrix adhesion. *J. Cell. Physiol.* **213**, 565-573.
- Choi, C. K., Zareno, J., Digman, M. A., Gratton, E. and Horwitz, A. R. (2011). Cross-correlated fluctuation analysis reveals phosphorylation-regulated paxillin-FAK complexes in nascent adhesions. *Biophys. J.* **100**, 583-592.
- Cluzel, C., Saltel, F., Lussi, J., Paulhe, F., Imhof, B. A. and Wehrle-Haller, B. (2005). The mechanisms and dynamics of α (v) β 3 integrin clustering in living cells. *J. Cell Biol.* **171**, 383-392.
- Deakin, N. O. and Turner, C. E. (2008). Paxillin comes of age. *J. Cell Sci.* **121**, 2435-2444.
- Digman, M. A., Brown, C. M., Sengupta, P., Wiseman, P. W., Horwitz, A. R. and Gratton, E. (2005). Measuring fast dynamics in solutions and cells with a laser scanning microscope. *Biophys. J.* **89**, 1317-1327.
- Edgington, E. S. (1995). *Randomization Tests*. New York, NY: Marcel Dekker, Inc.
- Eduardo, M., Lotano, M. A. and Otey, C. A. (2001). Dynamics of alpha-actinin in focal adhesions and stress fibers visualized with alpha-actinin-green fluorescent protein. *Cell Motil. Cytoskeleton* **48**, 190-200.
- Efron, B. and Tibshirani, R. J. (1993). *An Introduction to the Bootstrap*. New York, NY: Chapman and Hall.
- Essers, J., Houtsmuller, A. B., van Veelen, L., Paulusma, C., Nigg, A. L., Pastink, A., Vermeulen, W., Hoeijmakers, J. H. and Kanaar, R. (2002). Nuclear dynamics of RAD52 group homologous recombination proteins in response to DNA damage. *EMBO J.* **21**, 2030-2037.
- Ezratty, E. J., Partridge, M. A. and Gundersen, G. G. (2005). Microtubule-induced focal adhesion disassembly is mediated by dynamin and focal adhesion kinase. *Nat. Cell Biol.* **7**, 581-590.
- Farla, P., Hersmus, R., Geverts, B., Mari, P. O., Nigg, A. L., Dubbink, H. J., Trapman, J. and Houtsmuller, A. B. (2004). The androgen receptor ligand-binding domain stabilizes DNA binding in living cells. *J. Struct. Biol.* **147**, 50-61.
- Farla, P., Hersmus, R., Trapman, J. and Houtsmuller, A. B. (2005). Antiandrogens prevent stable DNA-binding of the androgen receptor. *J. Cell Sci.* **118**, 4187-4198.
- Geuijen, C. A. and Sonnenberg, A. (2002). Dynamics of the α 6 β 4 integrin in keratinocytes. *Mol. Biol. Cell* **13**, 3845-3858.
- Giannone, G., Rondé, P., Gaire, M., Beaudouin, J., Haiech, J., Ellenberg, J. and Takeda, K. (2004). Calcium rises locally trigger focal adhesion disassembly and enhance residency of focal adhesion kinase at focal adhesions. *J. Biol. Chem.* **279**, 28715-28723.
- Goffin, J. M., Pittet, P., Csucs, G., Lussi, J. W., Meister, J. J. and Hinz, B. (2006). Focal adhesion size controls tension-dependent recruitment of alpha-smooth muscle actin to stress fibers. *J. Cell Biol.* **172**, 259-268.
- Good, P. I. (2005). *Permutation, Parametric and Bootstrap Tests of Hypotheses*. New York, NY: Springer.
- Hamadi, A., Bouali, M., Dontenwill, M., Stoeckel, H., Takeda, K. and Rondé, P. (2005). Regulation of focal adhesion dynamics and disassembly by phosphorylation of FAK at tyrosine 397. *J. Cell Sci.* **118**, 4415-4425.
- Härdle, W., Horowitz, J. and Kreiss, J. P. (2003). Bootstrap methods for time series. *Int. Stat. Rev.* **71**, 435-459.
- Houtsmuller, A. B. (2005). Fluorescence recovery after photobleaching: application to nuclear proteins. *Adv. Biochem. Eng. Biotechnol.* **95**, 177-199.
- Houtsmuller, A. B. and Vermeulen, W. (2001). Macromolecular dynamics in living cell nuclei revealed by fluorescence redistribution after photobleaching. *Histochem. Cell Biol.* **115**, 13-21.
- Katz, B. Z., Zamir, E., Bershadsky, A., Kam, Z., Yamada, K. M. and Geiger, B. (2000). Physical state of the extracellular matrix regulates the structure and molecular composition of cell-matrix adhesions. *Mol. Biol. Cell* **11**, 1047-1060.
- Lele, T. P., Pendse, J., Kumar, S., Salanga, M., Karavitis, J. and Ingber, D. E. (2006). Mechanical forces alter zyxin unbinding kinetics within focal adhesions of living cells. *J. Cell. Physiol.* **207**, 187-194.
- Lele, T. P., Thodeti, C. K., Pendse, J. and Ingber, D. E. (2008). Investigating complexity of protein-protein interactions in focal adhesions. *Biochem. Biophys. Res. Commun.* **369**, 929-934.
- Li, S., Guan, J. L. and Chien, S. (2005). Biochemistry and biomechanics of cell motility. *Annu. Rev. Biomed. Eng.* **7**, 105-150.
- Mattern, K. A., Swiggers, S. J., Nigg, A. L., Löwenberg, B., Houtsmuller, A. B. and Zijlmans, J. M. (2004). Dynamics of protein binding to telomeres in living cells: implications for telomere structure and function. *Mol. Cell Biol.* **24**, 5587-5594.
- Möhl, C., Kirchgessner, N., Schäfer, C., Küpper, K., Born, S., Diez, G., Goldmann, W. H., Merkel, R. and Hoffmann, B. (2009). Becoming stable and strong: the interplay between vinculin exchange dynamics and adhesion strength during adhesion site maturation. *Cell Motil. Cytoskeleton* **66**, 350-364.
- Pasapera, A. M., Schneider, I. C., Rericha, E., Schlaepfer, D. D. and Waterman, C. M. (2010). Myosin II activity regulates vinculin recruitment to focal adhesions through FAK-mediated paxillin phosphorylation. *J. Cell Biol.* **188**, 877-890.
- Phair, R. D. and Misteli, T. (2001). Kinetic modelling approaches to *in vivo* imaging. *Nat. Rev. Mol. Cell Biol.* **2**, 898-907.
- Schaller, M. D., Hildebrand, J. D., Shannon, J. D., Fox, J. W., Vines, R. R. and Parsons, J. T. (1994). Autophosphorylation of the focal adhesion kinase, pp125FAK, directs SH2-dependent binding of pp60src. *Mol. Cell Biol.* **14**, 1680-1688.
- Turner, C. E. (2000a). Paxillin interactions. *J. Cell Sci.* **113**, 4139-4140.
- Turner, C. E. (2000b). Paxillin and focal adhesion signalling. *Nat. Cell Biol.* **2**, E231-E236.
- van de Water, B., Houtepen, F., Huigsloot, M. and Tijdens, I. B. (2001). Suppression of chemically induced apoptosis but not necrosis of renal proximal tubular epithelial (LLC-PK1) cells by focal adhesion kinase (FAK). Role of FAK in maintaining focal adhesion organization after acute renal cell injury. *J. Biol. Chem.* **276**, 36183-36193.
- van Royen, M. E., Farla, P., Mattern, K. A., Geverts, B., Trapman, J. and Houtsmuller, A. B. (2009). Fluorescence recovery after photobleaching (FRAP) to study nuclear protein dynamics in living cells. *Methods Mol. Biol.* **464**, 363-385.
- Webb, D. J., Parsons, J. T. and Horwitz, A. F. (2002). Adhesion assembly, disassembly and turnover in migrating cells — over and over and over again. *Nat. Cell Biol.* **4**, E97-E100.
- Webb, D. J., Brown, C. M. and Horwitz, A. F. (2003). Illuminating adhesion complexes in migrating cells: moving toward a bright future. *Curr. Opin. Cell Biol.* **15**, 614-620.
- Webb, D. J., Donais, K., Whitmore, L. A., Thomas, S. M., Turner, C. E., Parsons, J. T. and Horwitz, A. F. (2004). FAK-Src signalling through paxillin, ERK and MLCK regulates adhesion disassembly. *Nat. Cell Biol.* **6**, 154-161.
- Wolfenson, H., Lubelski, A., Regev, T., Klaffer, J., Henis, Y. I. and Geiger, B. (2009). A role for the juxtamembrane cytoplasm in the molecular dynamics of focal adhesions. *PLoS ONE* **4**, e4304.
- Yoshigi, M., Hoffman, L. M., Jensen, C. C., Yost, H. J. and Beckerle, M. C. (2005). Mechanical force mobilizes zyxin from focal adhesions to actin filaments and regulates cytoskeletal reinforcement. *J. Cell Biol.* **171**, 209-215.
- Zaidel-Bar, R., Cohen, M., Addadi, L. and Geiger, B. (2004). Hierarchical assembly of cell-matrix adhesion complexes. *Biochem. Soc. Trans.* **32**, 416-420.
- Zaidel-Bar, R., Itzkovitz, S., Ma'ayan, A., Iyengar, R. and Geiger, B. (2007a). Functional atlas of the integrin adhesome. *Nat. Cell Biol.* **9**, 858-867.
- Zaidel-Bar, R., Milo, R., Kam, Z. and Geiger, B. (2007b). A paxillin tyrosine phosphorylation switch regulates the assembly and form of cell-matrix adhesions. *J. Cell Sci.* **120**, 137-148.
- Zamir, E. and Geiger, B. (2001). Molecular complexity and dynamics of cell-matrix adhesions. *J. Cell Sci.* **114**, 3583-3590.